Article
Vol. 26, No. 6, p. 649–667, December 2022
https://doi.org/10.1007/s12303-022-0018-x
pISSN 1226-4806 eISSN 1598-7477
Geosciences Journal GJ

Confirmation of the Floian-Darriwilian (Lower to Middle Ordovician) hiatus in the Taebaek Group, Korea: integration of conodont biostratigraphy and sedimentology

Byung-Su Lee[1], Se Hyun Cho[2]*, Suk-Joo Choh[2], and Xunlian Wang[3]

[1]Department of Earth Science Education, Chonbuk National University, Jeonju 54896, Republic of Korea
[2]Department of Earth and Environmental Sciences, Korea University, Seoul 02841, Republic of Korea
[3]School of Earth Sciences and Resources, China University of Geosciences, Beijing 100083, China

ABSTRACT: An Ordovician depositional hiatus spanning the middle Floian to lower Darriwilian, estimated to represent a period of at least 3 Myr, is confirmed for the first time in the Taebaek Group, Korea, based on integrated conodont biostratigraphic and sedimentologic data. The conodont biozones of the uppermost Dumugol and lower Makgol formations are revised and redefined with presentation of a new biozonal framework, which contains, the *Serratognathus bilobatus* Biozone, the *Serratognathus extensus* Biozone, the *Paraserratognathus obesus* Biozone, and the *Tangshanodus tangshanensis* Biozone in ascending order. The hiatus lies within the barren interval between the middle Floian *Paraserratognathus obesus* Biozone and the early Darriwilian *Tangshanodus tangshanensis* Biozone. The unconformity surface is located at the boundary between the basal and lower members of the Makgol Formation, 1.5 meters above the base of the barren interval, on the basis of sedimentary evidence such as differences in the depositional and diagenetic features as well as a sharp contact between the two members with subaerial exposure feature including vuggy to channel pore and dolostone breccia. The barren interval above the hiatus is considered due to environmental factor: the peritidal condition is regarded unfavorable for inhabitation of conodont animals. The newly established Floian and Darriwilian conodont biozones and depositional hiatus within the lower Makgol Formation indicate that the Ordovician succession of the Taebaek Group is essentially an extension of that of the North China Block.

Key words: Ordovician, conodont biostratigraphy, Taebaeksan Basin, Makgol Formation

Manuscript received January 13, 2022; Manuscript accepted July 7, 2022

1. INTRODUCTION

The Lower to Middle Ordovician hiatus of the North China (Sino-Korean) Block has long been recognized prior to the 1950s (Lee, 1939; Weller, 1944). As An et al. (1983) established a framework of the Ordovician conodont biostratigraphy of North China, the magnitude and regional variation of the hiatus became clearer; the Lower Ordovician succession below the unconformity differs in age from late Tremadocian to late Floian depending on the region, and the hiatus is uniformly overlain by upper Floian deposits (An et al., 1983). The recent revision of the conodont biostratigraphy of North China demonstrated the age of the strata above the unconformity to be early Darriwilian, extending the duration of the hiatus to at least 2 Myr, from the earliest Dapingian to the early Darriwilian (Zhen et al., 2016; Wang et al., 2018; Zhang et al., 2019).

Previous stratigraphic and paleontologic studies have confirmed that this Lower to Middle Ordovician hiatus is traceable in the western, southern, and northern regions of North China (Meng et al., 1997; Wang et al., 2018). In the Taebaeksan Basin of Korea, which constitutes the easternmost margin of the North China Block, some sequence stratigraphic and sedimentologic works correlated the subaerial exposure features in the upper Makgol Formation of the Taebaek Group to this hiatus, but they have not been examined biostratigraphically (Ryu, 2002; Kwon et al., 2006). The conodont bioprovince from the Ordovician strata of the Taebaek Group has been postulated to be similar to that of

*Corresponding author:
Se Hyun Cho
Department of Earth and Environmental Sciences, Korea University, 145 Anam-ro, Seongbuk-gu, Seoul 02841, Republic of Korea
Tel: +82-10-5236-3394, Fax: +82-2-3290-3189,
E-mail: whtpgus307@korea.ac.kr

North China because of the co-occurrence of endemic species (Lee and Lee, 1986; Lee and Lee, 1990). This similarity is further complemented by the common occurrence of an Upper Ordovician to Carboniferous hiatus ('the Great hiatus') in North China and the Taebaeksan Basin (Lee et al., 2017; Cho et al., 2021), which has been well documented with detailed paleontologic review from the contact between the lower Paleozoic Joseon and upper Paleozoic Pyeongan supergroups (Chough, 2013; Lee et al., 2017).

A recent conodont biostratigraphic review of the Taebaek Group (Cho et al., 2021), which utilized the up-to-date North China conodont biostratigraphic scheme (Zhen et al., 2016; Wang et al., 2018; Xue et al., 2021) strongly suggested the presence of a previously overlooked Lower to Middle Ordovician hiatus within the lower part of Makgol Formation, similar to those reported across North China due to 'Huaiyuan epeirogeny' (Zhen et al., 2016; Wang et al., 2018). Unfortunately, clear biostratigraphic division of the lower Makgol Formation has not been possible, because of poor conodont recovery in previous studies (Lee, 1976; Hwang, 1986; Kim, 1987; Lee, 2009).

The aim of the present study is to re-establish the conodont biostratigraphy of the lower Makgol Formation in the Seokgaejae section and to provide the first clear evidence of the Lower to Middle Ordovician hiatus in the Taebaek Group, by integrating conodont biostratigraphy and sedimentary facies analysis.

2. GEOLOGICAL SETTING AND METHOD

The Taebaeksan Basin, located in the east-central Korean Peninsula, is composed of the lower Paleozoic Joseon Supergroup, which rests unconformably on the Precambrian basement and is overlain by the upper Paleozoic Pyeongan Supergroup (Fig. 1a). The mixed carbonate-clastic Joseon Supergroup is divided into five units, including the Taebaek, Yeongwol, Yongtan, Pyeongchang, and Mungyeong groups, on the basis of their geographic distributions (Chough, 2013). The Taebaek Group was deposited from Cambrian Epoch 2 to the Middle Ordovician and contains five Ordovician lithostratigraphic units, which are, in ascending order, the Dongjeom, Dumugol, Makgol, Jigunsan, and Duwibong formations (Choi et al., 2004; Chough, 2013). The recent review of conodont studies on these Ordovician

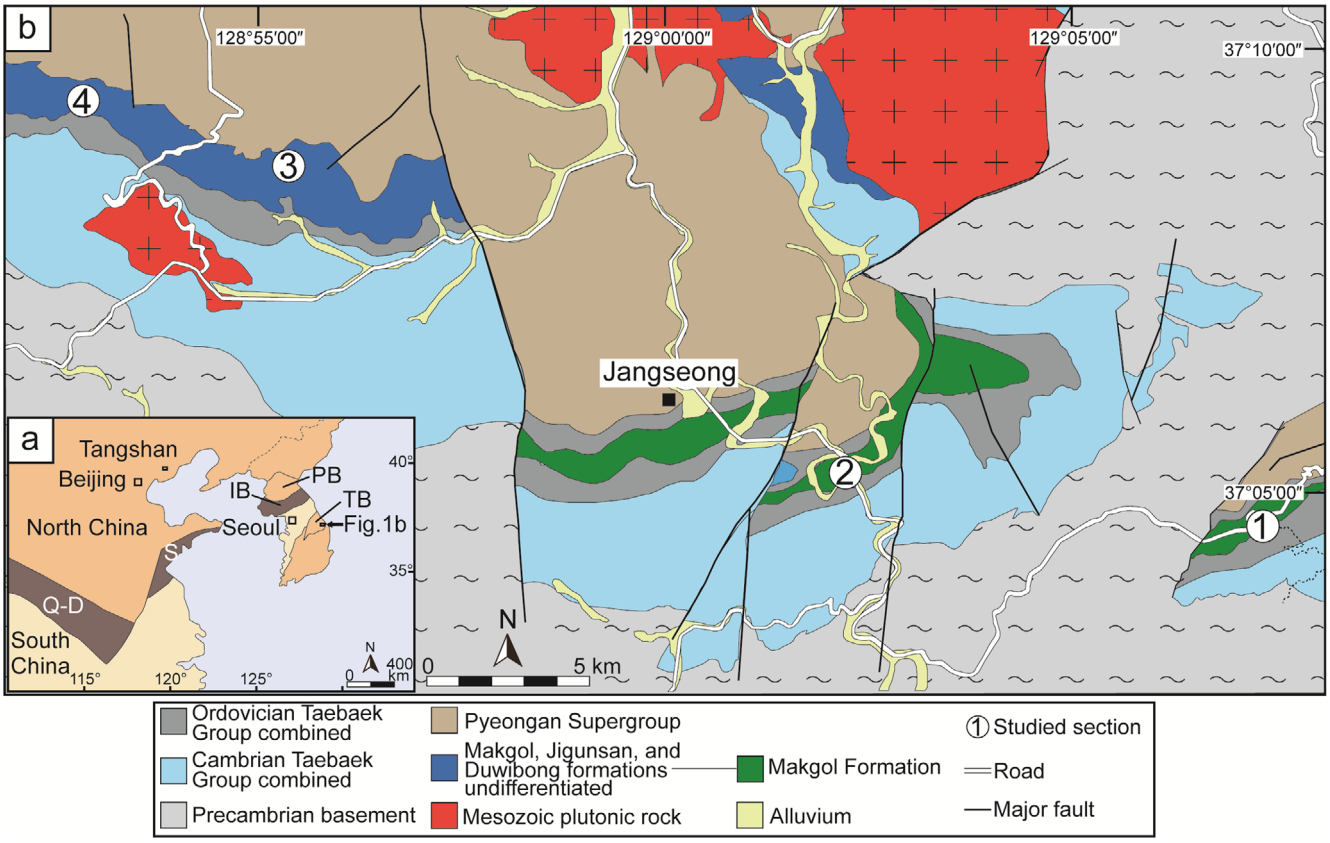

Fig. 1. (a) Tectonic map of the North China and South China blocks. IB, Imjingang Belt; PB, Pyeongnam Basin, Q-D, Qingling–Dabie Belt; S, Sulu Belt; TB, Taebaeksan Basin (modified after Chough, 2013, fig. 6.1). (b) Geologic map of the study area. 1, Seokgaejae section; 2, Gumunso section; 3, Hyeoldong section; 4, Sangdong section (modified after Chough et al., 2000, fig. 10).

strata indicated that the conodonts of the Dumugol Formation are late Tremadocian to earliest Floian in age; the middle Makgol to Duwibong formations contain middle Darriwilian forms; and middle Floian, Dapingian, and early Darriwilian conodonts have not been reported to date (Cho et al., 2021).

This study focuses on the lower Makgol Formation, which is crucial for resolving the Floian to lower Darriwilian conodont biostratigraphy in the Taebaek Group. The definition of the boundary between the Dumugol Formation and the overlying Makgol Formation varied in previous studies. Earlier studies defined the 60-meters-thick interval composed of limestone-shale couplets and sponge bioherms and the overlying 20- to 50-meters-thick massive dolostone interval as the lower and middle members of the Makgol Formation, respectively (Paik, 1987; Woo, 1999), whereas later works designated the base of the massive dolostone interval as the boundary between the two formations, and defined the underlying 60-meters-thick interval as the upper member of the Dumugol Formation (Choi et al., 2004; Kwon et al., 2006). Herein we follow the latter definition.

The four members of the Makgol Formation crop out at the Seokgaejae section (locality 1 in Fig. 1b) located in Bongwha-gun, Gyongsangbuk-do (Choi et al., 2004). They are the basal member dominated by massive dolostone, the lower member composed of grainstone-mudstone couplets, stromatolitic limestone, and bioturbated wackestone, the middle member consisting of massive dolostone and dolostone breccia, and the upper member which is lithologically similar to the lower member (Choi et al., 2004). A columnar section showing the depositional textures and sedimentary structures was drawn for the 150-meters-thick interval from the uppermost Dumugol Formation to the lower member of the Makgol Formation exposed in the Seokgaejae section (Fig. 2). In addition, the boundaries between the basal and lower members were described in detail in the Gumunso, Hyeoldong, and Sangdong sections (localities 2, 3, and 4 in Fig. 1b) to trace the horizontal extent and assess the vertical nature of the contact. A total of 607 hand specimens were collected, and thin sections were prepared from all samples for detailed description of composition and sedimentary structure. In the dolomitized samples, the "white card method" was used to recognize the primary depositional texture and components (Delgado, 1977).

To facilitate efficient conodont biostratigraphic analysis, samples for conodont extraction were selected based on depositional facies to maximize conodont recovery. Samples were primarily collected from the fossil-bearing bioturbated wackestone and bioclastic-intraclastic packstone to grainstone rather than the less fossiliferous lime mudstone and peloidal-ooidal grainstone (Fig. 2).

3. PREVIOUS WORK

3.1. Lithostratigraphy and Sedimentology

Early work on the stratigraphic and paleontologic framework of the Ordovician succession of the Taebaeksan Basin was carried out by Kobayashi (1934) nearly a century ago. Kobayashi (1934) defined the 'Makdong Limestone' (= the Makgol Formation) as a 400-meters-thick limestone-dominated unit, which overlies the 'Dumudong Shale' (= the Dumugol Formation) and is overlain by the 'Jigunsan Shale' (Kobayashi, 1966). The Makdong Limestone was informally subdivided into the lower part, composed of thin to platy limestone with the Arenig *Clarkella* (trilobite) biozone, and the upper part, composed of dark gray massive limestone (Kobayashi, 1966). Until the 1970s, there were few attempts to refine stratigraphy of the Joseon Supergroup (GICTR, 1962; Kim et al., 1973; Son, 1973). The present-day Makgol Formation of the Taebaek Group, as defined by Choi et al. (2004), is about 250-meters-thick succession consisting of dark gray massive dolostone, laminated dolomitic limestone, and dolostone breccia.

A few sedimentologic studies of the Makgol Formation were published since the 1980s. Paik (1987) divided the Makgol Formation into subtidal facies of oolitic-peloidal grainstone and peritidal facies of rhythmically bedded mudstone and stromatolite, and suggested that the overall depositional environment was a relatively humid tidal flat with occasional dry seasons. In addition, there were attempts to relate the depositional facies to diagenetic sequence (Paik, 1986, 1988). Woo (1999) recognized meter-scale cycles within the formation by describing vertical repetitions of subtidal and peritidal facies, and suggested overall climate change during deposition of the formation. Ryu (2002) and Kwon et al. (2006) placed a sequence boundary in the uppermost Makgol Formation based on the presence of subaerial exposure feature and carbonate breccia.

3.2. Previous Conodont Studies

Two papers (Lee, 1976; Lee and Lee, 1990) and three unpublished theses (Hwang, 1986; Kim, 1987; Lee, 2009) have reported the conodonts of the Makgol Formation. Lee (1976) subdivided the conodont assemblage into the lower and upper faunas based on 39 conodont species. The lower fauna was correlated with the middle to late Canadian (Floian) coeval fauna in North America and the upper fauna was compared with the North American Chazyan (late Darriwilian–early Sandbian) fauna.

Hwang (1986) studied the conodonts of the formation in Sangdong area (locality 4 in Fig. 1b), and defined (from oldest to youngest) the *Scalpellodus tersus* Biozone, the *Serratognathus bilobatus* Biozone, the *Scolopodus flexilis* Biozone, the *Aurilobodus*

https://doi.org/10.1007/s12303-022-0018-x

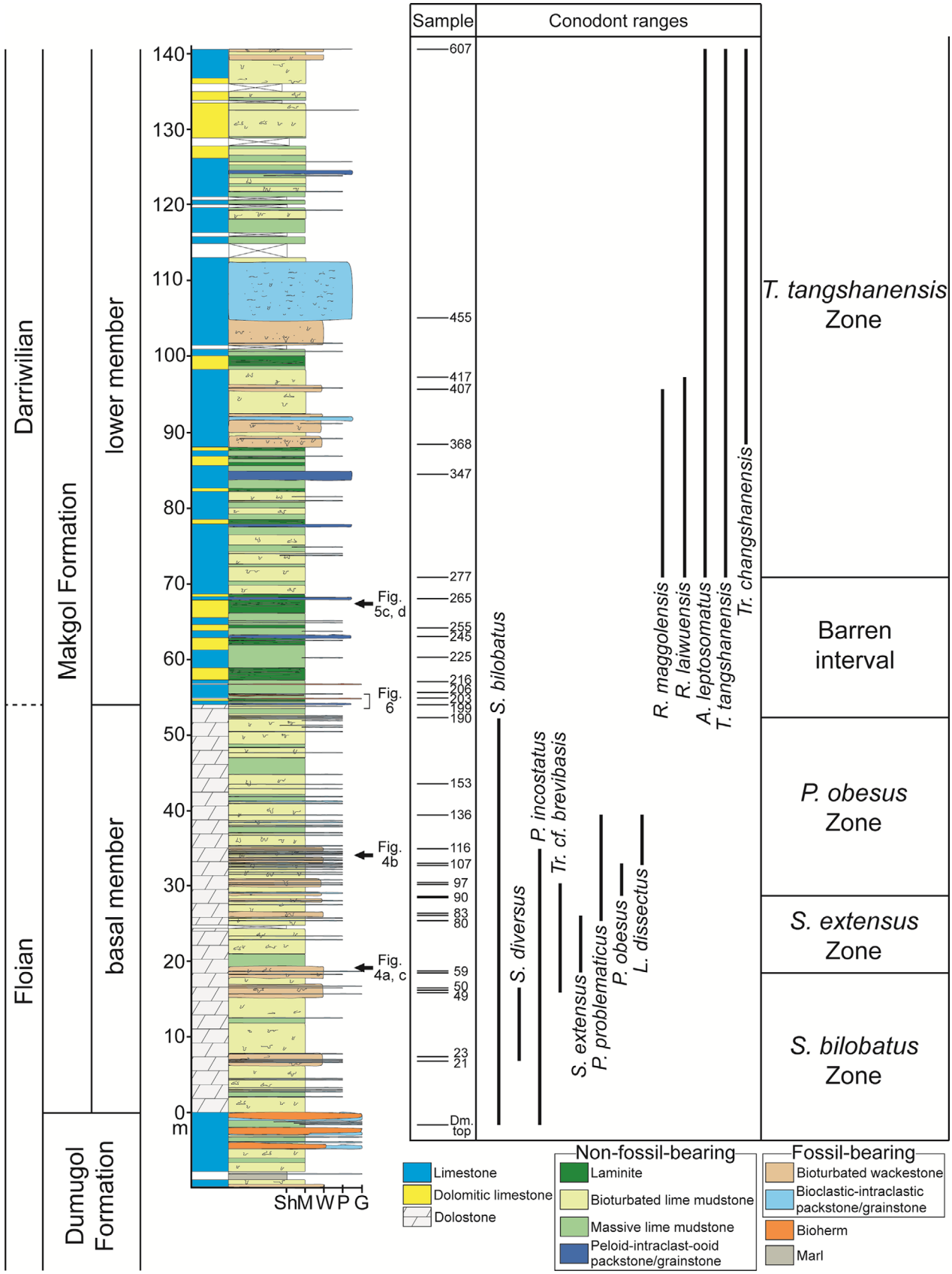

Fig. 2. Range chart of representative species from the uppermost Dumugol Formation and the basal and lower members of the Makgol Formation in the Seokgaejae section. Abbreviations of generic names: *A.* = *Aurilobodus*; *L.* = *Loxodus*; *P.* = *Paraserratognathus*; *R.* = *Rhipidognathus*; *S.* = *Serratognathus*; *T.* = *Tangshanodus*; *Tr.* = *Triangulodus*.

leptosomatus–Loxodus dissectus Biozone, and the Unnamed Zone. Similarly, Kim (1987) erected six biozones for the formation in the Taebaek and Yeongwol areas: the *Scalpellodus tersus* Biozone, Unnamed Zone A, the *Serratognathus diversus* Biozone, the *Aurilobodus leptosomatus–Loxodus dissectus* Biozone, the *Aurilobodus* n. sp.–*Tangshanodus tangshanensis* Biozone, and Unnamed Zone B in ascending order. Kim (1987) correlated these zones with those of the Liangjiashan Formation to lower Majiagou Formation (Arenigian to lower Llanvirnian [= upper Tremadocian to lowest Darriwilian]) of North China, with the Fauna D to Fauna 3 (Whiterockian [= lower Dapingian to middle Darriwilian]) of North America, and with the *Oepikodus evae* Biozone to *Paroistodus originalis* Biozone (Arenigian to lower Llanvirnian [= lower Floian to lower Darriwilian]) of northern Europe (Bergström, 1970; Sweet et al., 1970).

Lee and Lee (1990) defined two biozones, which are in ascending order, the *Aurilobodus leptosomatus* Biozone and the Unnamed Zone, in the upper Makgol Formation in Jangseong–Dongjeom area (locality 2 in Fig. 1b), and interpreted each of these biozones to represent a similar time span, as suggested by Hwang (1986).

Lee (2009) reported the conodonts of the formation in the Seokgaejae (locality 1 in Fig. 1b) and Sanaegol sections and established, in ascending order, the *Serratognathus bilobatus* Biozone, the *Tangshanodus tangshanensis–Rhipidognathus laiwuensis* Assemblage Biozone, and the Unnamed Zone, representing the early Arenigian to early Llanvirnian (= Floian to early Darriwilian) in age.

4. CONODONT OCCURRENCES

A total of 41 samples, each weighing approximately 2 kg, were collected for conodont extraction (Fig. 2). More than 77 kg of limestone and dolomitic limestone were processed in acetic acid using standard methods of conodont extraction (Stone and Austin, 1987). Thirty-two productive samples yielded 1,500 relatively well-preserved conodonts, an average of 47 specimens per sample. The most productive sample (19 meters above the base of the formation, sample 59; Fig. 2), from near the base of the *Serratognathus extensus* Biozone, yielded more than 133 specimens, about 8.9% of the total collection. Some conodont specimens are fragmentary and attached with foreign matter on their surfaces because of incomplete dissolution. Conodont color alteration index values range from 3 to 5, indicating burial temperatures of 110–200 °C to over 300 °C (Epstein et al., 1977).

Biostratigraphically significant conodonts include *Serratognathus bilobatus* Lee, 1970, *Serratognathus diversus* An in An et al., 1981, *Paraserratognathus incostatus* Yang and Lin in An et al., 1983, *Triangulodus* cf. *brevibasis* (Sergeeva, 1963), *Serratognathus extensus* Yang in An et al., 1983, *Paraserratognathus problematicus* Zhang and Yang in An et al., 1983, *Paraserratognathus obesus* Yang in An et al., 1983, *Loxodus dissectus* An in An et al., 1983, *Rhipidognathus maggolensis* (Lee, 1976), *Rhipidognathus laiwuensis* Zhang in An et al., 1983, *Aurilobodus leptosomatus* An in An et al., 1983, *Tangshanodus tangshanensis* An in An et al., 1983, and *Triangulodus changshanensis* Zhang in An et al., 1983 (Figs. 2 and 3).

5. CONODONT BIOSTRATIGRAPHY

The re-established conodont biozonation of the Seokgaejae section follows the current biostratigraphic scheme for North China (An et al., 1983; Wang et al., 2011; Wang et al., 2014a, 2014b; Zhen et al., 2016; Ma et al., 2019). We propose four conodont biozones based on Floian and Darriwilian key species: the *Serratognathus bilobatus* Biozone, the *Serratognathus extensus* Biozone, the *Paraserratognathus obesus* Biozone, barren interval, and the *Tangshanodus tangshanensis* Biozone in ascending order (Figs. 2 and 3).

5.1. *Serratognathus bilobatus* Biozone

The lower limit of the *Serratognathus bilobatus* Biozone is defined by the FAD of *Serratognathus bilobatus* Lee, 1970 in the uppermost Dumugol Formation (2 meters below the base of the Makgol Formation, Fig. 2). The upper limit is defined by the FAD of *Serratognathus extensus* Yang in An et al., 1983 of the lower basal member, 19 meters above the base of the Makgol Formation (Fig. 2). This biozone is an updated version of the previously established *S. bilobatus* Biozone in the Taebaek Group (Hwang, 1986; Lee, 2009) with the refined data for its lower and upper limits.

The dominant species in this biozone are *S. bilobatus*, *Serratognathus diversus* An in An et al., 1981, *Acodus cortinus* An in An et al., 1983, *Bergstroemognathus extensus* (Graves and Ellison, 1941), *Drepanodus homocurvatus* Lindström, 1955, *Drepanodus tenuis* Moskalenko, 1967, *Drepanoistodus concavus* (Branson and Mehl, 1933), *Drepanoistodus expansus* (Chen and Gong, 1986), *Glyptoconus quadraplicatus* (Branson and Mehl, 1933), *Oistodus inaequalis* Pander, 1856, *Oistodus lanceolatus* Pander, 1856, *Oistodus multicorrugatus* Harris, 1962, *Paraserratognathus incostatus* Yang and Lin in An et al., 1983, *Paroistodus proteus* (Lindström, 1955), *Rhipidognathus yichangensis* (Ni, 1981), *Scalpellodus tersus* Zhang in An et al., 1983, *Scandodus rectus* Lindström, 1955, *Scolopodus asperus* An in An et al., 1981, *Scolopodus rex huolianzhaiensis* An and Xu in An et al., 1983, and *Triangulodus* cf. *brevibasis* (Sergeeva, 1963).

S. bilobatus plays an important role in determining Early

https://doi.org/10.1007/s12303-022-0018-x

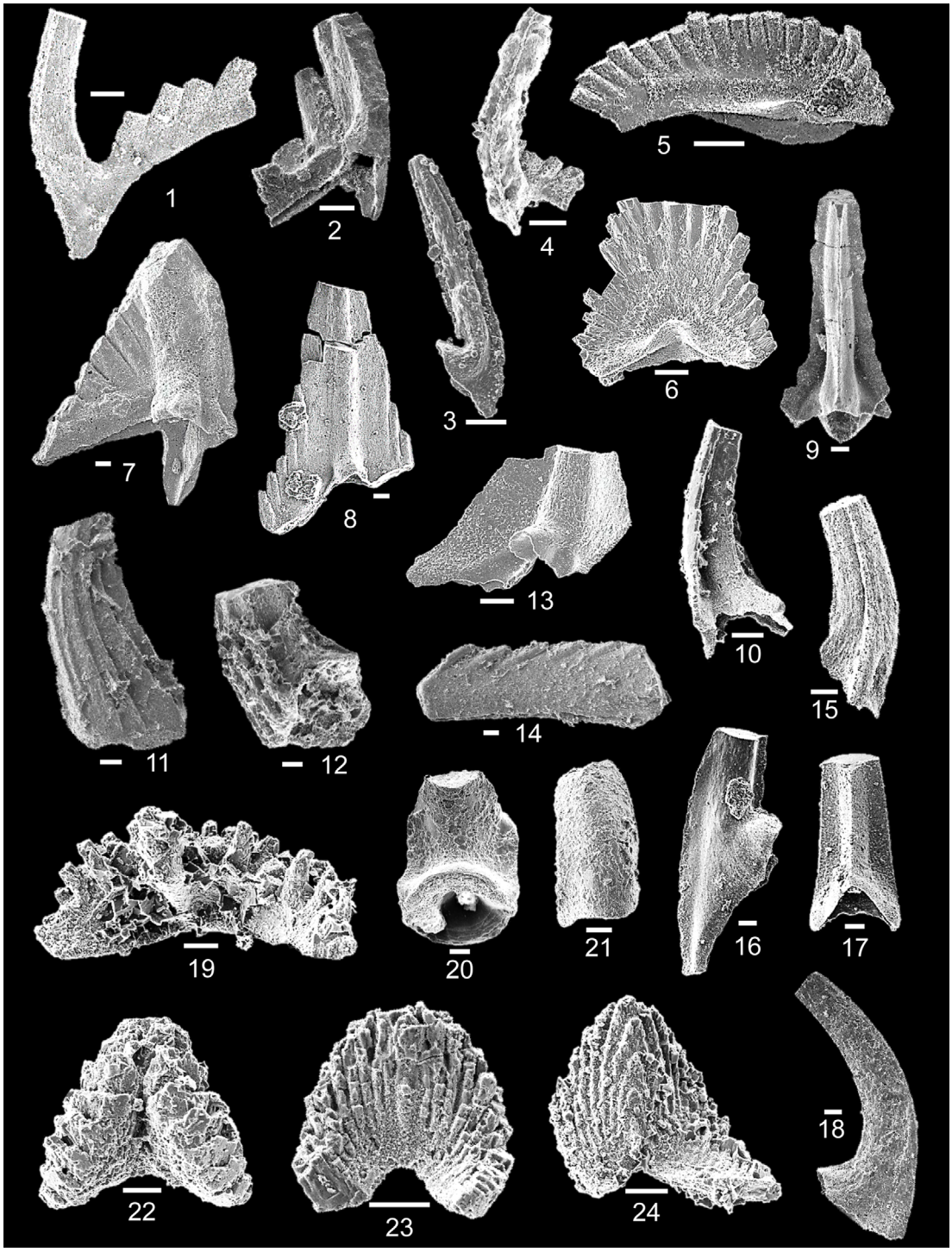

Fig. 3. Scanning electron micrographs of biostratigraphically useful conodonts from the Makgol Formation in the Seokgaejae section, Seokpo-ri, Bonghwa-gun, Korea. All scale bars are 0.1 millimeter. 1–4, *Tangshanodus tangshanensis* An in An et al., 1983; 1, Pb element, sample 407, lateral view; 2, Sd element, sample 455, lateral view; 3, M element, sample 417, lateral view; 4, Pb element, sample 407, lateral view. 5 and 6, *Rhipidognathus laiwuensis* Zhang in An et al., 1983; 5, Sb elements, sample 368, posterior views; 6, Sa element, posterior view, sample 277. 7 and 8, *Rhipidognathus maggolensis* (Lee, 1976); 7, Sc element, sample 368, posterior view; 8, Sb element, sample 368, posterior view. 9 and 10, *Triangulodus changshanensis* Zhang in An et al., 1983; 9, Sa element, sample 368, posterior view; 10, Sb element, sample 368, lateral view. 11, *Paraserratognathus problematicus* Zhang and Yang in An et al., 1983; S element, sample 97. 12, *Paraserratognathus obesus* Yang in An et al., 1983; S element, sample 107. 13, *Aurilobodus leptosomatus* An in An et al., 1983; Symmetrical element, sample 607, posterior view. 14, *Loxodus dissectus* An in An et al., 1983; P element, sample 107, inner lateral view. 15–18, *Triangulodus* cf. *brevibasis* (Sergeeva, 1963); 15, Sb element, sample 277, lateral view; 16, M element, sample 368, lateral view; 17, Sa element, sample 407, posterior view; 18, P element, sample 90, lateral view. 19, *Serratognathus extensus* Yang in An et al., 1983; Sa element, sample 83, posterior view. 20 and 21, *Paraserratognathus incostatus* Yang and Lin in An et al., 1983; 20, Sb element, sample 23, posterior view; 21, Sa element, sample 59, anterior view**.** 22 and 23, *Serratognathus bilobatus* Lee, 1970; Sb elements, sample 49. 24, *Serratognathus diversus* An in An et al., 1981; Sb element, sample 21, posterior view.

https://doi.org/10.1007/s12303-022-0018-x https://www.springer.com/journal/12303

Ordovician biostratigraphy and biogeography. Lee (1970) illustrated two specimens of *S. bilobatus* from the Dumugol Formation, with the holotype (Lee, 1970, pl. 8, figs. 7a–d) assignable to the asymmetrical Sb element and a paratype (Lee, 1970, pl. 8, fig. 6) being a symmetrical Sa element. In North China, *S. bilobatus* has been widely reported to occur in the Liangjiashan Formation, but is confined to the lower 30 m of the formation at Zhaogezhuang section (Hebei Province) (An et al., 1983, p. 26).

The *S. bilobatus* Biozone represents an interval of the early Floian in age, equivalent to the late *Paroistodus proteus* Biozone to earliest *Prioniodus elegans* Biozone of the Baltoscandian conodont succession, which typically indicates a lower-latitude warm-water realm (Zhen and Nicoll, 2009).

5.2. *Serratognathus extensus* Biozone

The base of the *Serratognathus extensus* Biozone is defined by the FAD of *Serratognathus extensus* Yang in An et al., 1983 at 19 meters above the base of the Makgol Formation (sample 59; Fig. 2). The upper limit is defined by the FAD of *Paraserratognathus obesus* Yang in An et al., 1983, 28 meters above the base of the formation (sample 90). This biozone established in North China typically include *Serratognathus bilobatus*, *Bergstroemognathus extensus* (Graves and Ellison, 1941), *Bergstroemognathus hubeiensis* An in An et al., 1981, *Cornuodus longibasis* Lindström, 1955, and *Oistodus multicorrugatus* Harris, 1962 (Wang et al., 2018). In the Makgol Formation, this biozone is dominated by three rhipidognathid species: *Rhipidognathus yichangensis* (Ni, 1981); *B. extensus*; and *B. hubeiensis*. In addition to these taxa, scolopodid species are also common. The presence of these species may be indicative of continuously shallowing marine environments.

The *S. extensus* Biozone of the Makgol Formation corresponds to the homonymous zone established in the lower Liangjiashan Formation to lower Majiagou Formation in the Liangjiashan section (Hebei Province) (Ma et al., 2019). An et al. (1983, p. 26) reported that this biozone extends through the middle part of the Liangjiashan Formation, with a total thickness of 50 meters. First defined in the Pingquan and Tangshan sections of Hebei Province (An et al., 1983), the *S. extensus* Biozone commonly occurs in the northern and western regions of North China (Wang et al., 2018); this is the first time that this biozone has been recorded in the Taebaeksan Basin.

5.3. *Paraserratognathus obesus* Biozone

This biozone is typified by the FAD of *Paraserratognathus obesus* Yang in An et al., 1983 in the middle part of the basal member of the Makgol Formation (28 meters above the base of the formation, sample 90). The *Paraserratognathus obesus* Biozone extends from this level to the uppermost basal member of the Makgol Formation (53 meters above the base of the formation, sample 190; Fig. 2) and the base of the barren interval.

The common conodonts in this biozone are *P. obesus*, *S. bilobatus*, *Paraserratognathus incostatus*, *Paraserratognathus problematicus*, *Cornuodus longibasis* Lindström, 1955, *Drepanodus suberectus* (Branson and Mehl, 1933), *Loxodus dissectus* An in An et al., 1983, *Paltodus inconstans* Lindström, 1955, *Scolopodus euspinus* Jiang and Zhang in An et al., 1983, and *Scolopodus restrictus* An in An et al., 1983, with some long-ranging species persisting from the underlying zones.

The *P. obesus* Biozone of the Makgol Formation corresponds to the *Paraserratognathus paltodiformis* Biozone (An et al., 1983), *Paraserratognathus obesus* Biozone (Wang et al., 2014b), and *Paraserratognathus obesus–Paraserratognathus paltodiformis* Biozone (Zhen et al., 2016) of the Liangjiashan Formation (Hebei and Liaoning provinces). This zone was first defined in the Tangshan section (Hebei Province) (Wang et al., 2014b); the present study is its first record in the Taebaeksan Basin.

5.4. Barren Interval

This interval is approximately 18 m thick, extending from the uppermost basal member (53 meters above the base of the formation, sample 190; Fig. 2) to the FAD of *Tangshanodus tangshanensis* An in An et al., 1983 at 71 meters above the base of the formation (lower member, sample 277). Except for *Serratognahtus bilobatus* from sample 190, only 13 poorly preserved elements were obtained from three (from sample 225, 245, and 255) of eight samples collected at this interval. The implications of the barren interval are discussed below.

5.5. *Tangshanodus tangshanensis* Biozone

The remainder of the examined interval of the Makgol Formation, from 71 to 140 meters above the base, is assigned to the *Tangshanodus tangshanensis* Biozone, though the upper boundary of the biozone is not present in the studied interval. This zone is defined by the FAD of *Tangshanodus tangshanensis*. Other associated taxa include *Rhipidognathus maggolensis* (Lee, 1976), *Rhipidognathus laiwuensis* Zhang in An et al., 1983, *Aurilobodus leptosomatus* An in An et al., 1983, *Triangulodus changshanensis* Zhang in An et al., 1983, *Scolopodus flexilis* An in An et al., 1981, *Drepanoistodus concavus* (Branson and Mehl, 1933), *Drepanodus arcuatus* Pander, 1856, *Oistodus lanceolatus* Pander, 1856, *Rhipidognathus yichangensis* (Ni, 1981), and *Scolopodus euspinus* Jiang and Zhang in An et al., 1983. This biozone combines the previously established *Aurilobodus leptosomatus–Loxodus dissectus* Biozone and the *Aurilobodus* n. sp.–*T.*

https://doi.org/10.1007/s12303-022-0018-x

tangshanensis Biozone (Kim, 1987), and replaces the *T. tangshanensis–R. laiwuensis* Assemblage Biozone (Lee, 2009) of the Makgol Formation. Wang et al. (2014a) erected the *Histiodella holodentata–T. tangshanensis* Biozone, based on the widely distributed species *Histiodella holodentata* Ethington and Clark, 1981 and the endemic species *T. tangshanensis* An in An et al., 1983 in the Bei'anzhuang Formation at the Zhaogezhuang section, Hebei Province. The *H. holodentata–T. tangshanensis* Biozone defined in the Bei'anzhuang Formation comprises the *Rhipidognathus maggolensis* and *Rhipidognathus laiwuensis* subzones, of which the latter is defined by the FAD of *R. laiwuensis* (Wang et al., 2014a). In the present study, however, *H. holodentata* was not recovered, and *T. tangshanensis*, *R. maggolensis*, and *R. laiwuensis* all firstly appear in sample 277 (71 meters above the base of the Makgol Formation; Fig. 2) at the base of the *T. tangshanensis* Biozone; thus, the subzonal division is not feasible in the Makgol Formation at present. Since *R. maggolensis* and *R. laiwuensis* have been reported from the *Serratognathus extensus* Biozone in the Liangjiashan Formation (Floian) of the Liangjiashan section (Hebei Province) (Ma et al., 2019), the subzonal division of *H. holodentata–T. tangshanensis* Biozone of North China should be reconsidered in future work.

6. ANATOMY OF THE LOWER TO MIDDLE ORDOVICIAN HIATUS

A recent review of the Taebaek Group Ordovician conodonts raised the possibility of a Lower to Middle Ordovician hiatus being present in the lower Makgol Formation, based on the absence of Floian, Dapingian, and early Darriwilian conodonts (Cho et al., 2021). In this study, newly acquired conodont data combined with sedimentologic data from four sections exposed in the Taebaek and Yeongwol regions confirm the presence of a formerly unrecognized gap in sedimentation. The temporal correlation of conodont zonation for estimating the depositional age and the duration of hiatus in the Makgol Formation follows the up-to-date Ordovician time scale (Goldman et al., 2020).

6.1. Paleontologic Evidence

The *Serratognathus bilobatus*, *Serratognathus extensus*, and *Paraserratognathus obesus* biozones range from the lower to middle Floian (Goldman et al., 2020). The *Tangshanodus tangshanensis* Biozone indicates the lower Darriwilian in up-to-date Ordovician time scale (Goldman et al., 2020), although previous studies have considered this biozone as a middle Darriwilian biozone (Zhen et al., 2016; Wang et al., 2018; Cho et al., 2021). Thus, the Makgol conodont faunas in this study collectively indicate the absence of late Floian to earliest Darriwilian conodonts, representing a hiatus within the barren interval, between the *P. obesus* and the *T. tangshanensis* biozones. In addition, the ongoing conodont study of the Makgol Formation at Cheoram (approximately 3 km northeast of Gumunso section) and Sangdong (locality 4 in Fig. 1b) sections reveal similar relationship to those of the Seokgaejae section; *P. obesus* and *T. tangshanensis* occur in the uppermost massive dolostone of basal member and the lower part of the lower member, respectively. The full range and content of all conodont species in Seokgaejae, Sangdong and Cheoram sections will be published somewhere else.

A recent review of Ordovician stratigraphy estimated the lower and upper boundaries of the *P. obesus* Biozone to be at ca. 475 and 472 Ma, respectively, and the lower and upper limits of the *H. holodentata–T. tangshanensis* Biozone in North China to be at approximately 469 and 465 Ma, respectively (Goldman et al., 2020). The minimum duration of the Makgol hiatus is estimated to be 3 Myr, given that the *P. obesus* and *T. tangshanensis* biozones are fully preserved, and the maximum could be 7 or 8 Myr, if the preservation of both biozones is considered minimal in the Seokgaejae section.

A Lower to Middle Ordovician hiatus has been recorded throughout North China, which is interpreted due to "Event 1" of the Huaiyuan Epeirogeny (Zhen et al., 2016). This event involved continuous vertical movement of North China Block during the late Cambrian to Middle Ordovician, and was recognized on the basis of extensive paleontologic and sedimentologic data, in particular, conodont studies (Zhang and Zhen, 1991; Chen et al., 2013; Wang et al., 2013a, 2013b, 2013c; Wang et al., 2014a, 2014b; Zhen et al., 2015, 2016).

The Makgol hiatus can be compared with global sea level trends. Global sea level curve of Haq and Schutter (2008) documented rising sea level during Early Ordovician, and falling stage in Middle Ordovician (the Dapingian to early Darriwilian). During Early–Middle Ordovician, short-term sea-level fall events were reported in Laurentia (Ross and Ross, 1995), Baltoscandia (Nielson, 2004), northern and western Gondwana (Ortega et al., 2007; Videt et al., 2010), and the duration of hiatus and re-inundation timing are different on each continent. The Middle Ordovician succession of Laurentia recorded the middle Floian–middle Darriwilian hiatus (Knox unconformity), and the overlying succession was initiated within the upper part of *Phragmodus polonicus* (conodont) Biozone, which could be correlated with the *Eoplacognathus suecicus* Biozone of North China and Taebaek Group (Read and Repetski, 2012; Taylor et al., 2012), thus younger than the Makgol Formation.

On the other hand, the Ordovician succession of the northern and western Gondwana and the Baltoscandia recorded transgressive

or drowning event during early Darriwilian, similar to the lower Makgol Formation (Nielson, 2004; Videt et al., 2010; Serra et al., 2018; Stouge et al., 2020). In the northern Gondwana, four third-order sequences and three Maximum Regressive Surfaces are described during Darriwilian: middle part of lower Darriwilian *Cyathochitina calix* (chitinozoan) Biozne, and middle and uppermost upper Darriwilian *Linochitina pissotensis* (chitinozoan) Biozone (Videt et al., 2010). Argentine Precordillera recorded black shale of Gualcamayo and Los Azules formations overlying thick fossiliferous carbonate of San Juan Formation with a diachronous transgressive event from the middle Dapingian *Isograptus victoriae maximus* (graptolite) Biozone to the lower Darriwilian *Levisograptus dentatus* (graptolite) Biozone (Ortega et al., 2007; Serra et al., 2018). Major transgressions of the Baltoscandia were reported in *Yangtzeplacognathus crassus* (conodont) Biozone (the 'basal Llanvirn Drowning event' of Nielson, 2004; the 'Tableheadian transgression' of Stouge et al., 2020), which can be correlated with *Tangshanodus tangshanensis* Biozone of the lower Makgol Formation.

6.2. Sedimentologic Evidence

6.2.1. Contrasting depositional character of the basal and lower members of the Makgol Formation

The barren interval is located between the uppermost basal member and the lower part of the lower member of the Makgol Formation (Fig. 2). These two members exhibit distinct differences in their sedimentary characteristics and depositional facies. The 54-meters-thick basal member of the Makgol Formation in the Seokgaejae section is characterized by "massive dolostone" in which the primary textures have been entirely overprinted by dolomitization (Choi et al., 2004). The basal member is mainly composed of dolomitized micritic facies such as massive or bioturbated dolomitic mudstone and bioturbated wackestone (Fig. 4a). The bioturbated dolo-micritic facies contains abundant horizontal to vertical burrows, with ichnofabric index 3–5 (Droser and Bottjer, 1986), and some trilobite and echinoderm fragments; rare brachiopod and mollusk remains and sponge spicules are also present. Very thin to thin beds of intraclastic

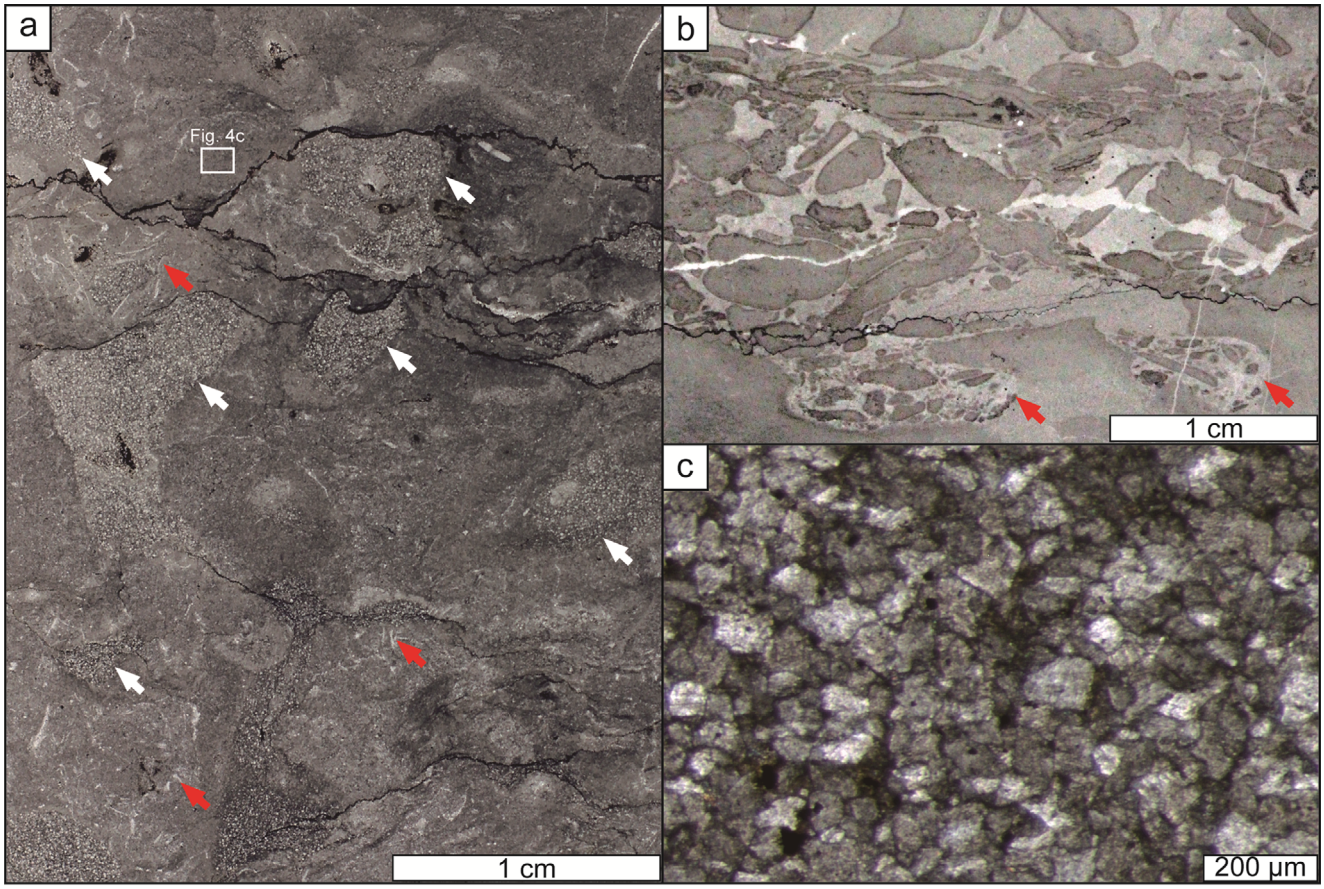

Fig. 4. Photomicrographs of the basal member of the Makgol Formation in the Seokgaejae section. (a) Bioturbated dolomitic mudstone with rare bioclasts (red arrows); the burrows (white arrows) are conspicuously filled by subhedral dolomite crystals. (b) Intraclastic packstone sharply overlying dolomitic mudstone with enlarged boring (red arrows). (c) Close-up of the white rectangle in (a); note that the dolomitic mudstone is composed of anhedral and subhedral dolomite crystals ranging 50 to 150 μm across.

https://doi.org/10.1007/s12303-022-0018-x

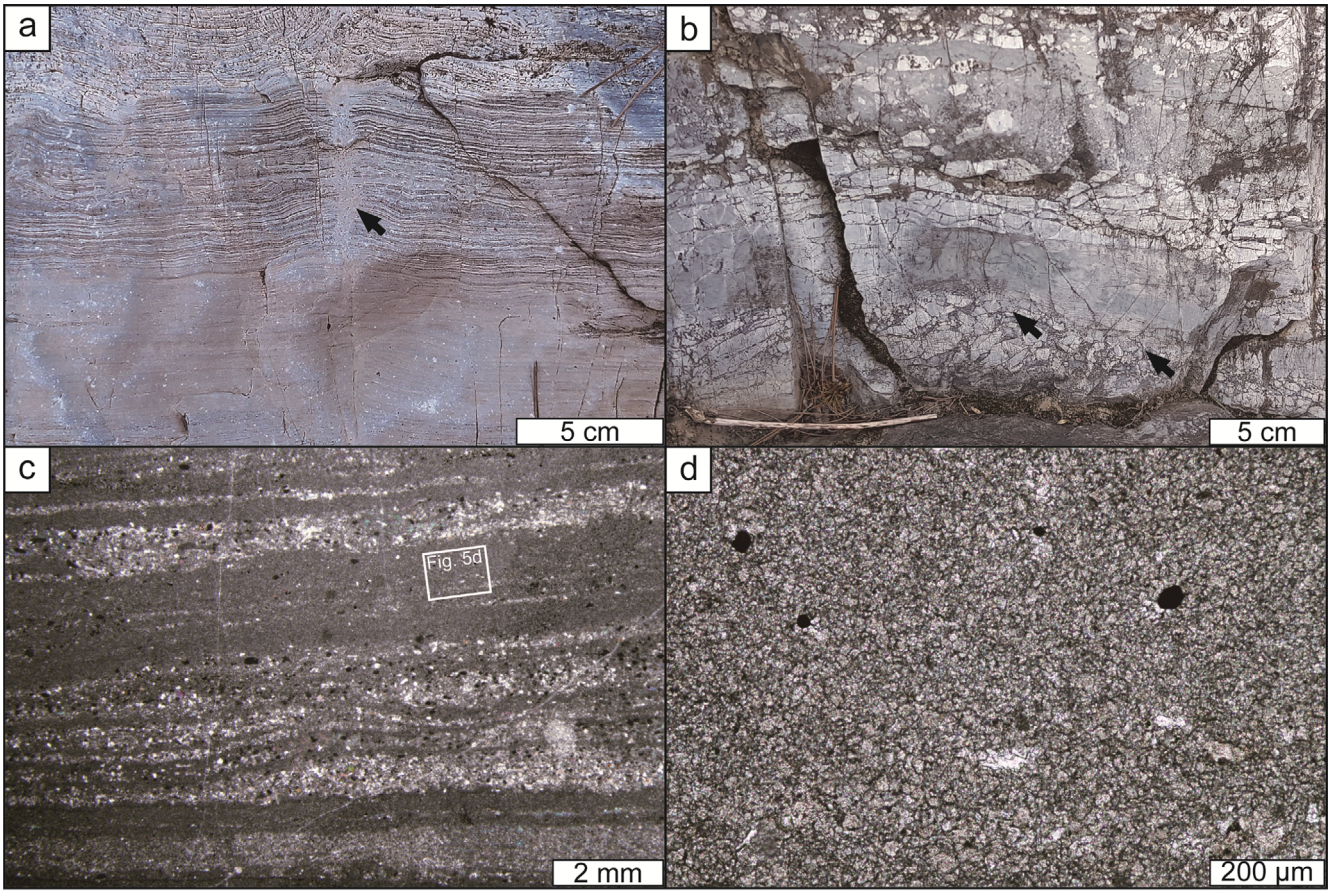

Fig. 5. Outcrop photographs and photomicrographs of the lower member of the Makgol Formation in Gumunso and Seokgaejae sections. (a) Laminite consisting of millimeter-scale alternations of dark and light layer, and a mud crack (black arrow) penetrating the laminae. (b) Carbonate breccia with jigsaw fit fabric (black arrows). (c) Photomicrograph of the laminite composed of alternative grainy layer and micritic layer. (d) Close-up of the rectangle in (c); note that the micritic layer consists of fine anhedral to subhedral dolomite crystals less than 20 μm in size.

packstone to grainstone with sharp lower boundaries are frequently intercalated within the unit, occurring more than eighty times within the basal member (Fig. 4b).

In the Seokgaejae section, the lower member of the Makgol Formation is 86-meters-thick, and is also dominated by micritic facies such as lime mudstone and wackestone (Fig. 2). However, the member is distinguished from the basal member by the occurrence of laminite consisting of millimeter-scale alternations of grainy and muddy sediment (Figs. 5a and c), stromatolites and thin beds (up to 3-centimeters-thick) of very coarse sandstone, and markedly lower frequency of intercalated intraclastic packstone to grainstone (36 very thin to thin beds and one medium bed in the interval). In addition, desiccation mud cracks, tepee structures, fenestrae pores, carbonate breccia, and pedogenic features are common in the lower member (Figs. 5a and b).

The dolo-micritic facies of the basal member, which contain burrows and bioclasts, with absence of subaerial exposure feature, is interpreted as having been deposited in a low-energy subtidal environment. The numerous interbedded intraclastic packstone to grainstone beds with sharp bases indicate the influence of frequent high-energy events such as storms (Àlvaro et al., 2000; Holland and Patzkowsky, 2009; Łabaj and Pratt, 2016). In contrast, the laminite of the lower member, which exhibits sedimentary structures such as desiccation mud cracks and fenestrae pores, is typical of a peritidal environment that is frequently affected by subaerial exposure (Shinn, 1983; Osleger and Montañez, 1996).

In addition to the differences in depositional feature and facies, there is a marked contrast in the style of dolomitization between the two members. The basal member is entirely overprinted by 50- to 400-μm anhedral to euhedral dolomite crystals, regardless of depositional texture and structure (Figs. 4c and 8b). These 20- to 50-meters-thick massive dolostones have been described in the Makgol Formation across the Yeongwol and Taebaek areas (Woo, 1999). In contrast, the dolomitic limestone beds of the lower member, which generally occur parallel to the bedding surface, are less than a few-meters-thick,

and are associated with laminite and immediately adjacent micritic facies. These dolomitic limestones are composed mostly of dolomite crystals less than 20 μm in size (Fig. 5d).

Several-meters-thick fine-grained dolostone of the lower member associated with peritidal facies appears to be related to synsedimentary evaporative dolomitization and/or repeated exposure related dolomitization (Coniglio et al., 1988; Lumsden and Caudle, 2001; Machel, 2004). However, widely distributed, several-tens of meters-thick coarse massive dolostone of the basal member may have been affected by a regional scale dolomitization process, which is distinctively different from that of the lower member. Tens to hundreds of meters-thick massive dolostone below the Early to Middle Ordovician hiatus has been reported throughout the North China Block (Liu et al., 1997; Li et al., 2022). This thick massive dolostone was interpreted as due to mixing zone or evaporative dolomitization associated with the unconformity based on the spatial change of dolostone bed thickness (Liu et al., 1997), or the combined effect of seepage reflux, burial and hydrothermal dolomitization was also suggested, based on isotopic and trace-element geochemical data (Li et al., 2022).

6.2.2. Contact between the basal and lower members

A recent work proposing the presence of hiatus based on biostratigraphic review of the Taebaek Group described a sharp and irregular boundary with subaerial exposure structures between the basal and lower members of the Makgol Formation in the Seokgaejae and Gumunso sections (Cho et al., 2021). In the present study, we confirm the existence of similar features at the boundary between the two members in the Hyeoldong and Sangdong sections (Figs. 6 and 7c). The massive dolostone below the sharp, irregular contact between the two members exhibits the textures of massive to bioturbated dolomitic mudstone and intraclastic packstone, and vuggy pores distributed parallel to the bedding surface are found in all sections (Fig. 6). In addition, laterally discontinuous, several-decimeters-thick dolostone-limestone breccia is present immediately below the contact in the Gumunso section (Figs. 6 and 7a). Except for the Sangdong section, this contact is overlain by a up to 50-centimeters-thick breccia composed of angular dolostone and limestone clasts with a micritic matrix containing well-rounded detrital quartz sand (Cho et al., 2021; Figs. 6, 7, 8a and c). In the Sangdong section, the basal member is immediately overlain by the laminite of the lower member (Fig. 6).

Petrographic analysis of a slab from the Seokgaejae section reveals the nature of the boundary in detail (Fig. 8). At the slab scale, the vuggy pores are interconnected with one another to form channel pores, which penetrate downward into the massive dolostone below the contact (Figs. 8a and b). These networks of pores are irregular in width and are partially filled with calcite cement, micrite, dolostone and limestone clasts, and quartz sand, similar to the dolostone-limestone breccia of the Gumunso

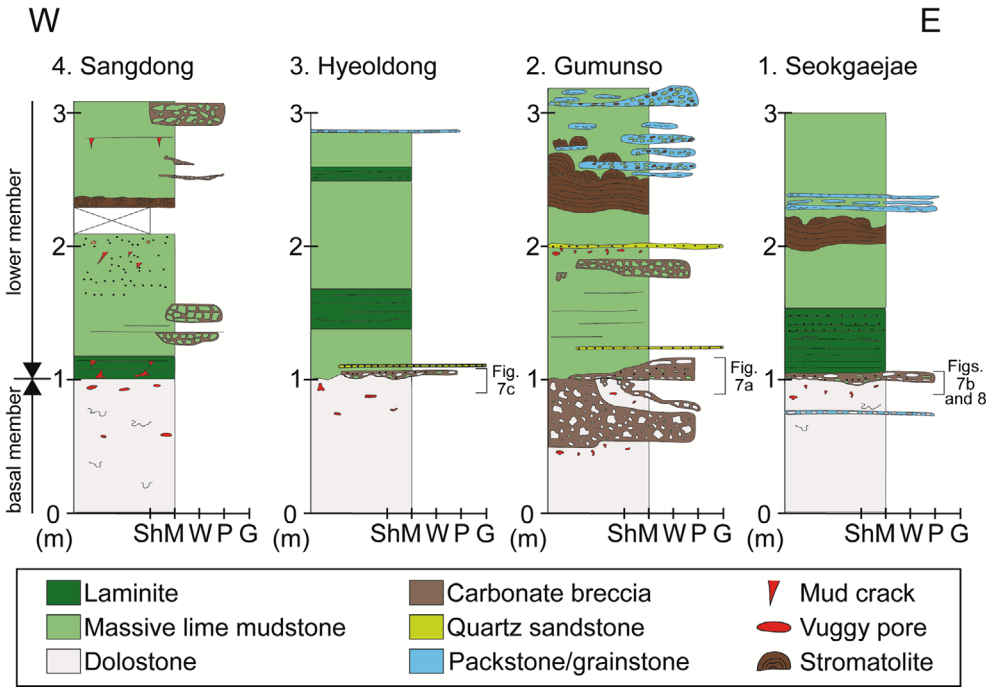

Fig. 6. Columnar sections of the uppermost basal member and lowest lower member of the Makgol Formation in the Sangdong, Hyeoldong, Gumunso, and Seokgaejae sections. The features of the boundary between two members, such as the irregularity of the contact and the distribution of carbonate breccia and vuggy pores, differ from section to section.

https://doi.org/10.1007/s12303-022-0018-x

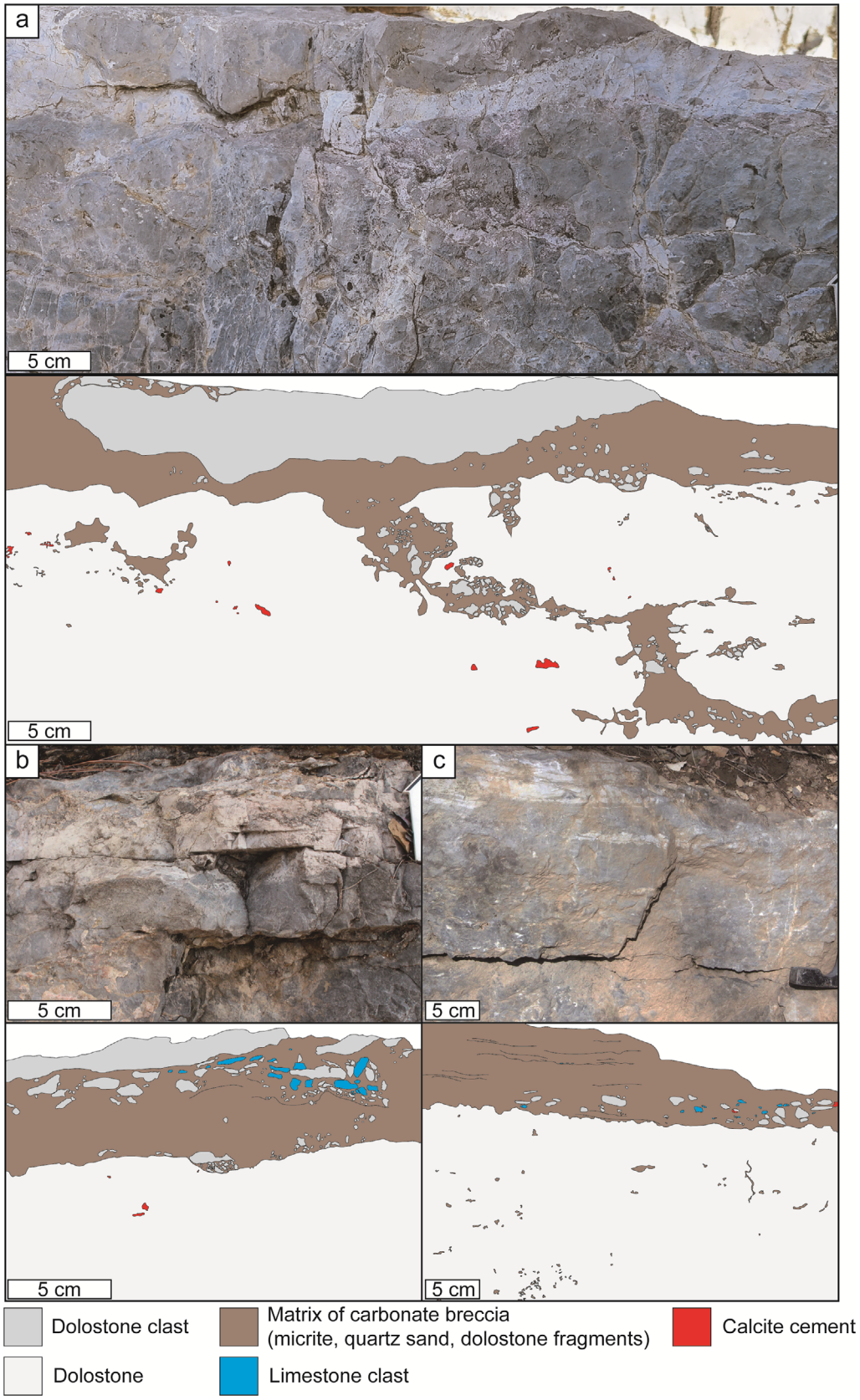

Fig. 7. Outcrop photograph and sketches showing the boundary between the basal and lower members of the Makgol Formation. (a), (b), and (c) are of the Gumunso, Seokgaejae, and Hyeoldong sections, respectively. Note the sharp, irregular contact between dark gray dolomitic mudstone and light gray lime mudstone. The dolomitic mudstone contains vuggy to channel pores filled by overlying micritic sediments, dolostone clasts, and calcite cement. The lime mudstone above the contact contains silt- to boulder-sized dolostone and limestone clasts.

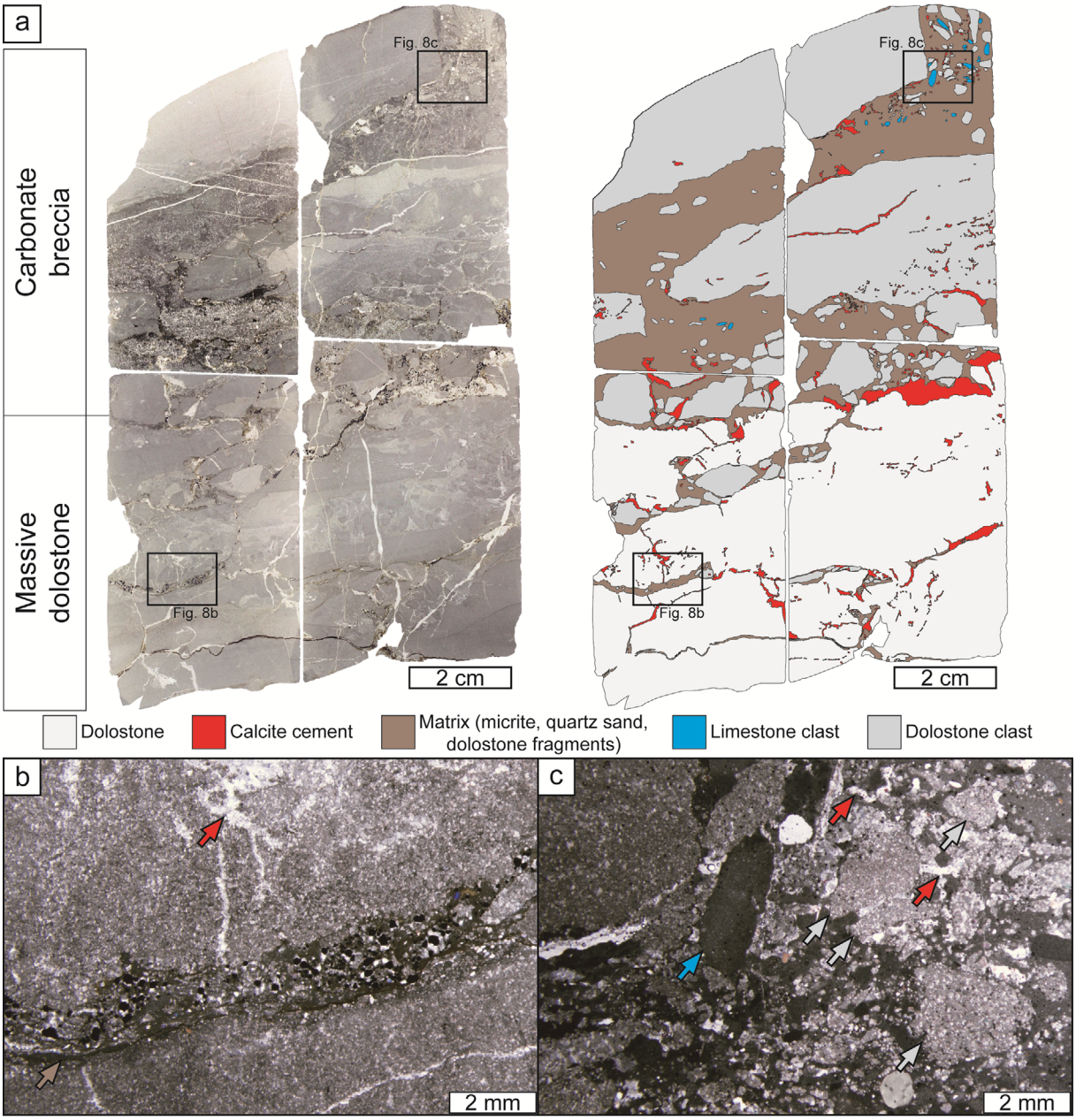

Fig. 8. Thin sections and photomicrographs of the boundary between the basal member and the lower member of the Makgol Formation in the Seokgaejae section. (a) Thin sections and sketch of the boundary; dolostone below the contact is penetrated by vuggy to channel pores, filled by dolostone clast, matrix, and calcite cement; carbonate breccia overlies dolostone with sharp and irregular contact. (b) Dolostone below the boundary composed of anhedral dolomite crystals, and penetrating channel pore filled by calcite cement (red arrow), or matrix consisting of micrite, fine sand-sized quartz grain and dolomite crystals. (c) Carbonate breccia above the boundary consisting of dolostone clast (grey arrows), limestone clast (blue arrows) and matrix of fine sand sized quartz and micrite with irregular vuggy pore (red arrows).

section (Figs. 7a, 8a and b). These dolostone/limestone clasts and quartz sand generally show a matrix-supported fabric, and tend to fill the lower parts of the pores forming geopetal fabric, with the remainder of the upper pore space filled with calcite cement. In some cases, dolostone clasts with vuggy pores show a jigsaw-fit fabric. Micritic matrix-supported breccia occurs immediately above the sharp contact, which is composed of dolostone and limestone clasts with micrite and quartz sand matrix (Figs. 7, 8a and c). The matrix is similar to the sediment infilling the channel pore networks below the contact, but with a higher proportion of micrite than the pore-filling sediments. The jigsaw-fit fabric around clasts is absent, and the dolostone clasts are of varying size (maximum tens of centimeters in length) and roundness. Limestone clasts generally show good roundness

https://doi.org/10.1007/s12303-022-0018-x

and smaller size (maximum 2-centimeters in length) than dolostone clasts (Fig. 8b). The vuggy to channel pores of various size and direction are also present above the sharp contact (Fig. 8c), and some pores are curved similar to those of the circumgranular cracks.

Features below the contact such as the downward penetration of channel pores with various directions and widths, which are partially filled with sediments from the overlying strata, can be interpreted as the result of dissolution and brecciation caused by subaerial exposure (Wright, 1983; Retallack, 2001). The jigsaw-fit fabric of the dolostone clasts in some pores indicates that the clasts were not transported; this texture is considered to form by in situ fragmentation (Chow and Wendte, 2011). In contrast, the matrix-supported breccia above the contact does not exhibit characteristics of in situ fragmentation and contains dolostone clasts that originated from the underlying massive dolostone interval, surrounded by micrite and rounded limestone clasts. This breccia is interpreted to represent post-unconformity sediments (Mussman and Read, 1986; Knight et al., 1991). The vuggy to channel pores above the sharp contact indicate that these sediments were affected by subaerial exposure during or after deposition.

6.2.3. The barren interval

Facies-specific sampling method adapted in this study enabled the establishment of the *Serratognathus extensus* and *Paraseratognathus obesus* biozones in the basal member of the Makgol Formation, which previous conodont studies failed to accomplish (Lee, 1976; Hwang, 1986; Kim, 1987; Lee, 2009). Nevertheless, few conodonts were recovered from the lower part of the lower member. The conodont barren interval above the hiatus is also recognized in the northern (Tangshan, Hebei Province) and southern (Laiwu, Shandong Province) regions of North China where several-tens of meters-thick conodont barren interval between the Early to Middle Ordovician hiatus and the FAD of *H. holodentata* is present (An et al., 1983; Wang et al., 2014a).

We suggest that poor conodont recovery in the barren interval is closely related to the depositional facies. All conodont-rich samples from the Makgol Formation were obtained from bioclast-bearing wackestone to packstone or bioturbated lime mudstone facies. In contrast, the barren interval is composed of peritidal facies of laminite, stromatolites, and massive lime mudstone with subaerial exposure features including mud cracks, tepee structures, and carbonate breccia (Fig. 2). This relationship between poor conodont recovery and specific depositional facies is consistent with paleoecologic studies suggesting that conodont community distribution was influenced by factors in the depositional environment (Heckel and Baesemann, 1975; Ji and Barnes, 1994; Zhang and Barnes, 2004). The lack of conodonts in the barren interval indicates that a peritidal environment was unfavorable for conodont animals compared to an open-marine subtidal environment (Ji and Barnes, 1994). A sedimentologic study of northern North China (Pingquan, Hebei Province) also described peritidal facies occurring above the hiatus (Liu and Zheng, 1998), suggesting that comparable conodont barren interval in other regions of North China was likely to have been influenced by the depositional environment, similarly to the Makgol Formation.

7. IMPLICATIONS FOR THE ORDOVICIAN SUCCESSION OF THE TAEBAEKSAN BASIN

In the Taebaek Group, the Lower to Middle Ordovician conodonts have been reported from the Dumugol to Duwibong formations. The Tremadocian conodont biozonation is relatively well established in the Dumugol Formation, and there is a Darriwilian zonal scheme for the lower member of the Makgol Formation upward into the Duwibong Formation (Lee and Lee, 1986; Lee and Lee, 1990; Seo et al., 1994; Seo and Lee, 2010). In contrast, the Floian and Dapingian conodonts have not been recorded in the Taebaek Group, except for the lowest Floian conodont *Serratognathus bilobatus* from the upper Dumugol Formation (Hwang, 1986), and accordingly, biozonal scheme has not been resolved for the uppermost Dumugol Formation and the basal member of the Makgol Formation. In the present study, we establish the middle Floian conodont biostratigraphy of the Taebaek Group and confirm the presence of a depositional hiatus based on the absence of certain biozones.

The new biozonation of the Makgol Formation allows revision of the Ordovician succession of the Taebaek Group based on the conodont biostratigraphy (Fig. 9). The scheme for the Taebaek Group is strikingly similar to the conodont biostratigraphy of North China in terms of the overall biozonation and the presence of two hiatuses, including 'the Great Hiatus' within the Ordovician strata (Zhen et al., 2016; Lee et al., 2017; Wang et al., 2018). The uppermost biozone of the Taebaek Group is the *Aurilobodus serratus* Biozone (Lee and Lee, 1986; Lee and Lee, 1990; Fig. 9). In northern North China, the upper limit of the Ordovician strata lies within the middle Darriwilian *Eoplacognathus suecicus* Biozone (An et al., 1983; Wang et al., 2014a), which differs from the southern and western regions containing the Sandbian and Katian strata (An et al., 1983; Wang et al., 2016; Wang et al., 2018). In addition, the temporal magnitude of the Early–Middle Ordovician hiatus, and the presence of the barren interval above the hiatus all collectively indicate that the revised Ordovician biostratigraphy of the Taebaek Group is consistent with that of the northern region of North China (Zhen et al., 2016; Wang et al., 2018).

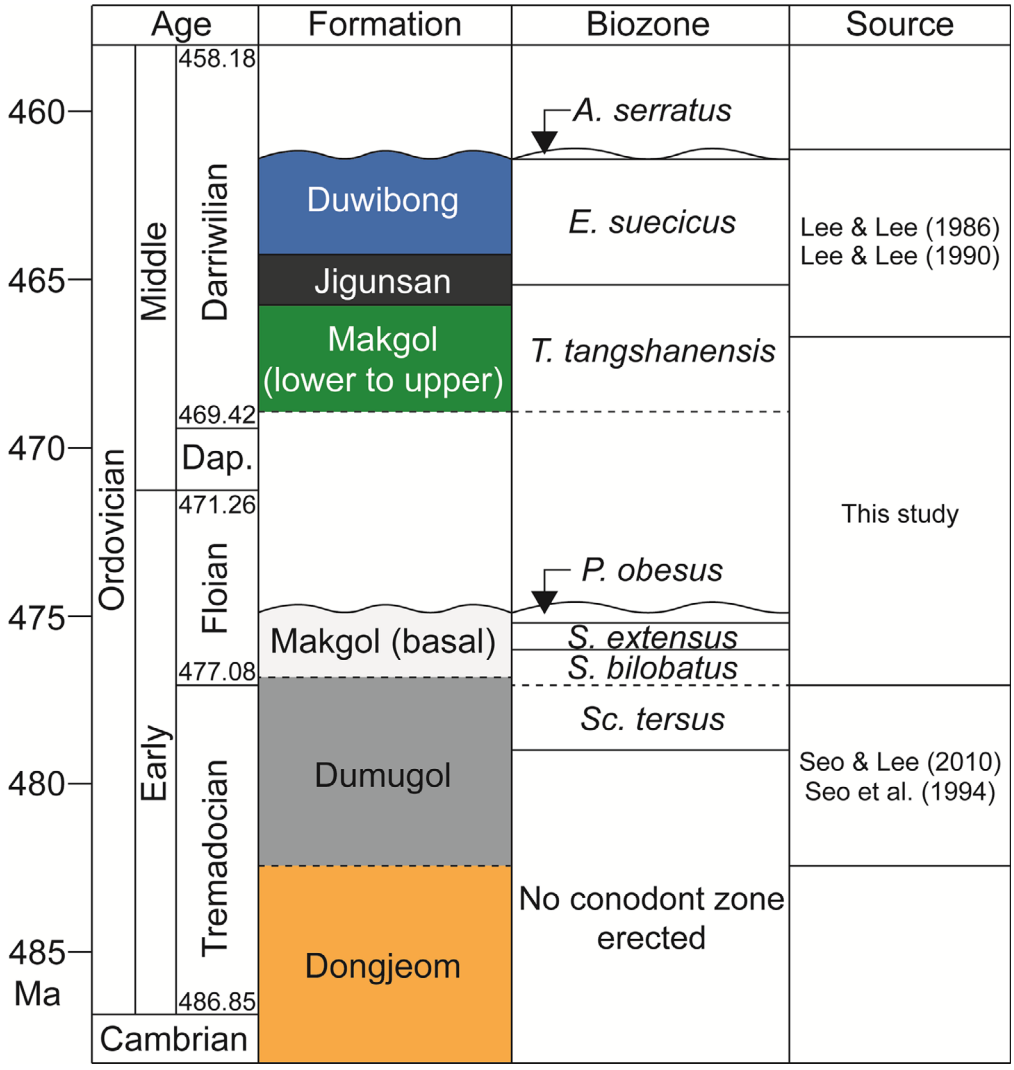

Fig. 9. Conodont biostratigraphic summary of the Taebaek Group to include the newly established biozones of the lower Makgol Formation. Radiometric ages are from Goldman et al. (2020). Dap. = Dapingian. Abbreviations of generic names: *A.* = *Aurilobodus*; *E.* = *Eoplacognathus*; *P.* = *Paraserratognathus*; *S.* = *Serratognathus*; *Sc.* = *Scalpellodus*; *T.* = *Tangshanodus*.

A similar approach is also warranted to revise biostratigraphy of other units in the Taebaeksan Basin. In the Yeongwol Group, a biostratigraphic study of the Mungok Formation reported the lowest Ordovician conodont *Cordylodus lindstromi* Druce and Jones, 1971 and Tremadocian conodonts such as *Rossodus manitouensis* Repetski and Ethington, 1983, *Chosonodina herfurthi* Müller, 1964, and *Glyptoconus quadraplicatus* (Branson and Mehl, 1933) (Lee and Lee, 1999). The immediately overlying Yeongheung Formation includes Darriwilian conodonts such as *Aurilobodus leptosomatus* An in An et al., 1983, *Erraticodon tangshanensis* Yang and Zu in An et al., 1983, *Plectodina onychodonta* An and Xu in An et al., 1983, and *Triangulodus changshanensis* Zhang in An et al., 1983 (Lee, 1990), but conspicuously, the Floian and Dapingian conodonts have not been reported to date, as shown by this study for the Taebaek Group.

8. CONCLUSIONS

This study confirms the presence of a Floian to early Darriwilian hiatus in the easternmost North China Block and it is the first biostratigraphic evidence of a previously unrecognized hiatus in South Korea. The Lower to Middle Ordovician conodont biostratigraphy of the Makgol Formation in the Seokgaejae section, Taebaeksan Basin, is re-established based on the recently updated conodont biostratigraphic scheme of North China, and can be correlated with successions throughout North China. Four conodont biozones are proposed: the lower to middle Floian *Serratognathus bilobatus*, *Serratognathus extensus*, and *Paraserratognathus obesus* biozones, and the lower Darriwilian *Tangshanodus tangshanensis* Biozone, with a barren interval between the *P. obesus* and *T. tangshanensis* biozones.

https://doi.org/10.1007/s12303-022-0018-x

The gap between the uppermost *P. obesus* Biozone and the barren interval represents a short-lived (at least 3 Myr) sedimentation hiatus, which is also corroborated by sedimentologic evidence such as difference of depositional feature and dolomitization style between basal and lower members of the Makgol Formation, and the sharp, irregular contact between the two members containing subaerial exposure features such as channel pore networks and breccia. The barren interval is considered to reflect peritidal depositional condition that were not favorable for conodont inhabitation. The revised conodont biostratigraphy of the lower Makgol Formation reveals that the Ordovician succession of the Taebaek Group is the extension of that of the northern region of the North China Block.

ACKNOWLEDGMENTS

This research was funded by National Research Foundation of Korea grants to BSL (2020R1A2C1099624) and to SJC (2021R1A2C1009687). We deeply appreciate careful review by J.-H. Lee (Chungnam National University), an anonymous reviewer and the editor D.C. Lee (Chungbuk National University) which considerably improved the manuscript.

REFERENCES

Àlvaro, J.J., Vennin, E., Moreno-Eiris, E., Perejón, A., and Bechstädt, T., 2000, Sedimentary patterns across the Lower-Middle Cambrian transition in the Esla nappe (Cantabrian Mountains, northern Spain). Sedimentary Geology, 137, 43–61.

An, T.X., Du, G.Q., Gao, Q.Q., Chen, X.B., and Li, W.T., 1981, Ordovician conodont biostratigraphy of the Huanghuachang area of Yichang, Hubei. Selected Papers of the 1st Convention of Micropalaeontological Society of China, Science Press, Beijing, p. 105–113. (in Chinese)

An, T.X., Zhang, F., Xiang, W.D., Zhang, Y.Q., Xu, W.H., Zhang, H.J., Jiang, D.B., Yang, C.S., Lin, L.D., Cui, Z.T., and Yang, X.C., 1983, The Conodonts of North China and the Adjacent Regions. Science Press, Beijing, 233 p. (in Chinese with English abstract)

Bergström, S.M., 1970, Conodont biostratigraphy of the Middle and Upper Ordovician of Europe and eastern North America. In: Sweet, W.C. and Bergström, S.M. (eds.), Symposium on Conodont Biostratigraphy. Geological Society of America Memoirs, 127, p. 83–162.

Branson, E.B. and Mehl, M.G., 1933, Conodonts from the Jefferson City (Lower Ordovician) of Missouri. University of Missouri Studies, 8, 53–64.

Chen, J.-Y. and Gong, W.-L., 1986, Conodonts. In: Chen, J. (ed.), Aspects of Cambrian–Ordovician Boundary in Dayangcha, China. China Prospect Publishing House, Beijing, p. 93–223.

Chen, X., Bergström, S.M., Zhang, Y.D., and Wang, Z.H., 2013, A regional tectonic event of Katian (Late Ordovician) age across three major blocks of China. China Science Bulletin, 58, 4292–4299.

Cho, S.H., Lee, B.-S., Lee, D.-J., and Choh, S.-J., 2021, The Ordovician succession of the Taebaek Group (Korea) revisited: old conodont data, new perspectives, and implications. Geosciences Journal, 25, 417–431.

Choi, D.K., Chough, S.K., Kwon, Y.K., Lee, S.B., Woo, J., Kang, I., Lee, H.S., Lee, S.M., Sohn, Y.J., and Lee, D.-J., 2004, Taebaek Group (Cambrian–Ordovician) in the Seokgaejae section, Taebaeksan Basin: a refined lower Paleozoic stratigraphy in Korea. Geosciences Journal, 8, 125–151.

Chough, S.K., 2013, Geology and Sedimentology of the Korean Peninsula. Elsevier, London, 363 p.

Chough, S.K., Kwon, S.-T., Ree, J.-H., and Choi, D.K., 2000, Tectonic and sedimentary evolution of the Korean peninsula: a review and new view. Earth-Science Reviews, 52, 175–235.

Chow, N. and Wendte, J., 2011, Palaeosols and paleokarst beneath subaerial unconformities in an Upper Devonian isolated reef complex (Judy Creek), Swan Hills Formation, west-central Alberta, Canada. Sedimentology, 58, 960–993.

Coniglio, M., James, N.P., and Aissaoui, D.M., 1988, Dolomitization of Miocene carbonates, Gulf of Suez, Egypt. Journal of Sedimentary Research, 58, 100–119.

Delgado, F., 1977, Primary textures in dolostones and recrystallized limestone: a technique for their microscopic study. Journal of Sedimentary Research, 47, 1339–1341.

Droser, M.L. and Bottjer, D.J., 1986, A semiquantitative field classification of ichnofabric. Journal of Sedimentary Petrology, 56, 558–559.

Druce, E.C. and Jones, P.J., 1971, Cambro-Ordovician conodonts from the Burke River structural belt, Queensland. Australian Bureau of Mineral Resources Bulletin, Geology and Geophysics, 110, 158 p.

Epstein, A.G., Epstein, J.B., and Harris, L.D., 1977, Conodont color alteration—an index to organic metamorphism. USGS Professional Paper, U.S. Geological Survey, 995, 27 p.

Ethington, R.L. and Clark, D.L., 1981, Lower and Middle Ordovician conodonts from the Ibex Area Western Millard County, Utah. Brigham Young University Geology Studies, 28, 1–159.

GICTR (Geological Investigation Crops of the Taebaegsan Region), 1962, Report on the Geology and Mineral Resources of the Taebaegsan Region. Geological Society of Korea, Seoul, 89 p.

Goldman, D., Sadler, P.M., Leslie, S.A., Melchin, M.J., Agterberg, F.P., and Gradstein, F.M., 2020, The Ordovician Period. In: Gradstein, F.M., Ogg, J.G., Schmitz, M.D., and Ogg, G.M. (eds.), The Geologic Time Scale 2020. Elsevier, Amsterdam, p. 631–694.

Graves, R.W. and Ellison, S., 1941, Ordovician conodonts of the Marathon Basin, Texas. University of Missouri, School of Mines and Metallurgy, Bulletin, 14, 1–26.

Haq, B.U. and Schutter, S.R., 2008, A Chronology of Paleozoic sea-level changes. Science, 322, 64–68.

Harris, R.W., 1962, New conodonts from the Joins (Ordovician) Formation of Oklahoma. Oklahoma Geology Notes, 22, 199–211.

Heckel, P.H. and Baesemann, J.F., 1975, Environmental interpretation of conodont distribution in Upper Pennsylvanian (Missourian) Megacyclothems in Eastern Kansas. American Association of Petroleum Geologists Bulletin, 59, 486–509.

Holland, S.M. and Patzkowsky, M.E., 2009, The stratigraphic distribution of fossils in a tropical carbonate succession: Ordovician big-

horn dolomite, Wyoming, USA. Palaios, 24, 303–317.
Hwang, I.S., 1986, Stratigraphic and micropaleontologic study on the Makgol Formation in the Sangdong area. M.Sc. Thesis, Yonsei University, Seoul, 75 p. (in Korean with English abstract) https://library.yonsei.ac.kr/search/detail/CAT000000355069
Ji, Z. and Barnes, C.R., 1994, Conodont paleoecology of the Lower Ordovician St. George Group, Port au Port Peninsula, western Newfoundland. Journal of Paleontology, 68, 1368–1383.
Kim, O.J., Lee, H.Y., Lee, D.S., and Yun, S., 1973, The stratigraphy and geologic structure of the Great Limestone Series in South Korea. Economic and Environmental Geology, 6, 81–114.
Kim, S.H., 1987, A study on stratigraphy and paleontology of the Maggol Limestone distributed in the south part of the Baegunsan Syncline – chiefly by means of conodont study. M.Sc. Thesis, Yonsei University, Seoul, 105 p. (in Korean with English abstract) https://library.yonsei.ac.kr/search/detail/CAT000000374244
Knight, I., James, N.P., and Lane, T.E., 1991, The Ordovician St. George Unconformity, northern Appalachians: the relationship of plate convergence at the St. Lawrence Promontory to the Sauk/Tippecanoe sequence boundary. Geological Society of America Bulletin, 103, 1200–1225.
Kobayashi, T., 1934, The Cambro-Ordovician formations and faunas of South Chosen. Palaeontology Part I. Middle Ordovician faunas. Journal of the Faculty of Science, University of Tokyo, 3, 329–519.
Kobayashi, T., 1966, Stratigraphy of the Chosen Group in Korea and South Manchuria and its relations to the Cambro-Ordovician formations of other area, Section D, The Ordovician of eastern Asia and other parts of the continent. Journal of Faculty of Science, University of Tokyo, 17, 163–316.
Kwon, Y.K., Chough, S.K., Choi, D.K., and Lee, D.J., 2006, Sequence stratigraphy of the Taebaek Group (Cambrian-Ordovician), mideast Korea. Sedimentary Geology, 192, 19–55.
Łabaj, M.A. and Pratt, B.R., 2016, Depositional dynamics in a mixed carbonate-siliciclastic system: Middle–Upper Cambrian Abrigo Formation, southeastern Arizona, U.S.A. Journal of Sedimentary Research, 86, 11–37.
Lee, B.-S. and Lee, J.D., 1999, Conodonts from the Mungog Formation (Lower Ordovician), Yeongwol. Journal of the Paleontological Society of Korea, 15, 21–42.
Lee, D.C., Choh, S.J., Lee, D.J., Ree, J.H., Lee, J.H., and Lee, S.B., 2017, Where art thou "great hiatus? – review of Late Ordovician to Devonian fossil-bearing strata in the Korean Peninsula and its tectonostratigraphic implications. Geosciences Journal, 21, 913–931.
Lee, H.Y., 1970, Conodonten aus der Chosen-Gruppe (Unteres Ordovizium) von Korea. Neues Jahrbuch für Geologie und Paläontologie Abhandelungen, 136, 303–344.
Lee, H.Y., 1976, Conodonts from the Maggol and the Jeongseon formations (Ordovician), Kangweon-Do, South Korea. Journal of Geological Society of Korea, 12, 151–182.
Lee, J.S., 1939, The geology of China. Thomas Murby and Co., London, 529 p.
Lee, K.W. and Lee, H.Y., 1990, Conodont biostratigraphy of the upper Choseon Supergroup in Jangseong–Dongjeom area, Gangweondo. Journal of the Paleontological Society of Korea, 6, 188–210.
Lee, S.J., 1990, Conodont biostratigraphy and paleontology of the Lower Paleozoic Youngheung Formation in the Yeongweol Area, Kangweondo, Korea. M.Sc. Thesis, Yonsei University, Seoul, 107 p. (in Korean with English abstract)
Lee, Y.N. and Lee, H.-Y., 1986, Conodont biostratigraphy of the Jigunsan shale and Duwibong limestone in the Nokjeon-Sangdong area, Yeongweol-gun, Kangweondo, Korea. Journal of the Paleontological Society of Korea, 2, 114–136.
Lee, Y.T., 2009, Classification of conodonts and biostratigraphy of the Makgol Formation in the Seokgaejae area, Kangweon-do. M.Sc. Thesis, Gongju National University, Gongju, 75 p. (in Korean with English abstract) http://www.riss.kr/link?id=T11545984
Li, F., Ma, X., and Lai, X., 2022, Petrography, geochemistry and genesis of dolomites in the upper Cambrian Sanshanzi Formation of the western Ordos Basin, northern China. Journal of Asian Earth Sciences, 223, 104980.
Lindström, M., 1955, Conodonts from the lowermost Ordovician strata of south-central Sweden. Geologiska Föreningens I Stockholm Förhandlingar, 76, 517–604.
Liu, B., Wang, Y., and Qian, X., 1997, Two Ordovician unconformities in North China: their origins and relationships to regional carbonate-reservoir characteristics. Carbonate and Evaporites, 12, 177–184.
Liu, J. and Zheng, Z., 1998, Stacking patterns and correlation of meter-scale shallowing-upward cycles in the Lower Ordovician carbonates in Pingquan and Qinglongshan, North China. Journal Geological Society of Japan, 104, 327–345.
Lumsden, D.N. and Caudle, C., 2001, Origin of massive dolostone: the upper Knox model. Journal of Sedimentary Research, 71, 400–409.
Ma, K., Li, R., Hinnov, L.A., and Gong, Y., 2019, Conodont biostratigraphy and astronomical tuning of the Lower–Middle Ordovician Liangjiashan (North China) and Huanghuachang (South China) marine sections. Palaeogeography, Palaeoclimatology, Palaeoecology, 528, 272–287.
Machel, H.G., 2004, Concepts and models of dolomitization: a critical reappraisal. In: Braithwaite, C.J.R., Rizzi, G., and Darke, G. (eds.), The Geometry and Petrogenesis of Dolomite Hydrocarbon Reservoirs. Geological Society, London, Special Publications, 235, p. 7–63.
Meng, X., Ge, M., and Tucker, M.E., 1997, Sequence stratigraphy, sea-level changes and depositional systems in the Cambro-Ordovician of the North China carbonate platform. Sedimentary Geology, 114, 189–222.
Moskalenko, T.A., 1967, Conodonts from the lower Chunsk beds, River Moiero and lower Stony Tunguska: new data on the biostratigraphy of the lower Paleozoic of the Siberian Platform. Academy of Sciences of the USSR, Siberian Division, 504, 98–116. (in Russian)
Müller, K.J., 1964, Conodonten aus dem unteren ordovizium von Sudkorea. Neues Jahrbuch für Geologie und Palaontologie Abhandlungen, 119, 93–102.
Mussman, W.J. and Read, J.F., 1986, Sedimentology and development of a passive- to convergent-margin unconformity: Middle Ordovician Knox unconformity, Virginia Appalachians. Geological Society of America Bulletin, 97, 282–295.
Ni, S.Z., 1981, Discussion on some problems of Ordovician stratigraphy by means of conodonts in eastern part of Yangtze Gorges Region. Selected Papers of the 1st Convention of Micropalaeontological Society of China, Science Press, Beijing, p. 127–134. (in Chinese)

https://doi.org/10.1007/s12303-022-0018-x

Nielson, A.T., 2004, Ordovician sea level changes: a Baltoscandian perspective. In: Webby, B.D., Paris, F., Droser, M.L., and Percival, I.G. (eds.), The Great Ordovician Biodiversification Event. Columbia University Press, New York, p. 84–93.

Ortega, G., Albanesi, G.L., and Frigerio, S.E., 2007, Graptolite-conodont biostratigraphy and biofacies of the Middle Ordovician Cerro Viejo succession, San Juan Precordillera, Argentina. Palaeogeography, Palaeoclimatology, Palaeoecology, 245, 245–263.

Osleger, D.A. and Montañez, I.P., 1996, Cross-platform architecture of a sequence boundary in mixed siliciclastic-carbonate lithofacies, Middle Cambrian, southern Great Basin, USA. Sedimentology, 43, 197–217.

Paik, I.S., 1986, Dolomitization of the Middle Ordovician Maggol Formation in Jangseong area, Gangweondo, Korea. Journal of the Geological Society of Korea, 22, 333–346.

Paik, I.S., 1987, Depositional environments of the Middle Ordovician Maggol Formation, southern part of the Baegunsan Syncline area. Journal of the Geological Society of Korea, 23, 360–373.

Paik, I.S., 1988, Diagenesis of the Middle Ordovician Maggol grainstones and pebble conglomerates, Jangseong, Kangwondo, Korea. Journal of the Geological Society of Korea, 24, 329–339.

Pander, C.H., 1856, Monographie der fossilen Fische des Silurischen Systems der Russisch-Baltischen Gouvernements. Kaiserlichen Akademie der Wissenschaften, St. Petersburg, 91 p.

Read, J.F. and Repetski, J.E., 2012, Cambrian–lower Middle Ordovician passive carbonate margin, southern Appalachians. In: Derby, J., Fritz, R., Longacre, S., Morgan, W., and Sternbach, C. (eds.), Great American Carbonate Bank: The Geology and Economic Resources of the Cambrian–Ordovician Sauk Megasequence of Laurentia. American Association of Petroleum Geologists Memoir, 98, p. 357–382. https://doi.org/10.1306/13331499M980271

Repetski, J.E. and Ethington, R.L., 1983, *Rossodus manitouensis* (conodonta), a new Early Ordovician index fossil. Journal of Paleontology, 57, 289–301.

Retallack, G.J., 2001, Soils of the Past: An Introduction to Paleopedology. Blackwell Science, Oxford, 404 p.

Ross, C.A. and Ross, J.R.P., 1995, North American Ordovician depositional sequences and correlations. In: Cooper, J.D., Droser, M.L., and Finney, S.C. (eds.), Ordovician Odyssey: Short Papers for the Seventh International Symposium on the Ordovician System. Society of Economic Paleontologists and Mineralogists Pacific Section, Fullerton, 77, p. 309–313.

Ryu, I.-C., 2002, Tectonic and stratigraphic significance of the Middle Ordovician carbonate breccias in the Ogcheon Belt, South Korea. The Island Arc, 11, 149–169.

Seo, K.-S. and Lee, B.-S., 2010, Conodonts from the Early Ordovician Dumugol Formation in Seckgaejae area, Bonghwagun, Kyunsangbukdo, Korea. Journal of the Paleontological Society of Korea, 26, 59–69. (in Korean with English abstract)

Seo, K.-S., Lee, H.-Y., and Ethington, R.L., 1994, Early Ordovician conodonts from the Dumugol Formation in the Baegunsan Syncline, eastern Yeongweol and Samcheog areas, Kangweon-do, Korea. Journal of Paleontology, 68, 599–616.

Sergeeva, S.P., 1963, Conodonts from the Lower Ordovician of the Leningrad region. Paleontologicheskiy Zhurnal, 1963, 93–108.

Serra, F., Feltes, N.A., Ortega, G., and Albanesi, G.L., 2018, Lower middle Darriwilian (Ordovician) graptolites and index conodonts from the Central Precordillera of San Juan Province, Argentina. Geological Journal, 53, 2161–2177.

Shinn, E.A., 1983, Tidal flat environment. In: Scholle, P.A., Bebout, D.G., and Moore, C.H. (eds.), Carbonate Depositional Environments. American Association of Petroleum Geologists Memoir, 33, p. 172–210.

Son, C.M., 1973, A discussion on the stratigraphy of the so-called Great Limestone Series. Economic and Environmental Geology, 6, 219–230.

Stone, J. and Austin, R.L., 1987, Review of investigative techniques used in the study of conodonts. In: Austin, R.L. (ed.), Conodonts: Investigative Techniques and Applications. Ellis Horwood Limited, Chichester, p. 17–34.

Stouge, S., Bagnoli, G., and Rasmussen, J.A., 2020, Late Cambrian (Furongian) to mid-Ordovician euconodont events on Baltica: invasions and immigrations. Palaeogeography, Palaeoclimatology, Palaeoecology, 549, 109151.

Sweet, W.C., Ethington, R.L., Barnes, C.R., and Bergström, S.M., 1970, North American Middle and Upper Ordovician conodont faunas. In: Sweet, W.C. and Bergström, S.M. (eds.), Symposium on Conodont Biostratigraphy. Geological Society of America Memoirs, 127, p. 163–193.

Taylor, J.F., Repetski, J.E., Loch, J.D., and Leslie, S.E., 2012, Biostratigraphy and chronostratigraphy of the Cambrian–Ordovician great American carbonate bank. In: Derby, J.R., Fritz, R.D., Longacre, S.A., Morgan, W.A., and Sternbach, C.A. (eds.), The Great American Carbonate Bank: The Geology and Economic Resources of the Cambrian–Ordovician Sauk Megasequence of Laurentia. American Association of Petroleum Geologists Memoir, 98, p. 15–35.

Videt, B., Paris, F., Rubino, J.-L., Boumendjel, K., Dabard, M.-P., Loi, A., Ghienne, J.-F., Marante, A., and Gorini, A., 2010, Biostratigraphical calibration of third order Ordovician sequences on the northern Gondwana platform. Palaeogeography, Palaeoclimatology, Palaeoecology, 296, 359–375.

Wang, Z.H., Bergström, S.M., Zhen, Y.Y., Chen, X., and Zhang, Y.D., 2013a, On the integration of Ordovician conodont and graptolite biostratigraphy: new examples from Gansu and Inner Mongolia in China. Alcheringa, 37, 510–528.

Wang, Z.H., Bergström, S.M., Zhen, Y.Y., and Zhang, Y.D., 2013b, New discovery of conodonts from the Upper Ordovician Pingliang Formation of Pingliang, Gansu, China and its significance. Acta Micropalaeontologica Sinica, 30, 123–131. (in Chinese with English abstract)

Wang, Z.H., Bergström, S.M., Zhen, Y.Y., Zhang, Y.D., and Wu, R.C., 2014a, A revision of the Darriwilian biostratigraphic conodont zonation in Tangshan, Hebei Province based on new conodont collections. Acta Palaeontologica Sinica, 53, 1–15. (in Chinese with English abstract)

Wang, Z.H., Bergström, S.M., Zhen, Y.Y., Zhang, Y.D., and Wu, R.C., 2014b, New conodont data from the Lower Ordovician of Tangshan, Hebei Province, North China. Acta Micropalaeontologica Sinica, 31, 1–14. (in Chinese with English abstract)

Wang, Z.H., Bergström, S.M., Zhen, Y.Y., Zhang, Y.D., Wu, R.C., and

Chen, Q., 2013c, Ordovician conodonts from Dashimen, Wuhai in Inner Monglolia and the significance of the discovery of the Histiodella fauna. Acta Micropalaeontologica Sinica, 30, 323–343. (in Chinese with English abstract)

Wang, Z.H., Qi, Y.P., and Wu, R.C., 2011, Cambrian and Ordovician Conodonts in China. Press of University of Science and Technology of China, Hefei, 388 p.

Wang, Z.H., Zhen, Y.Y., Bergström, S.M., Zhang, Y.D., and Wu, R.C., 2018, Ordovician conodont biozonation and biostratigraphy of North China. Australasian Palaeontological Memoirs, 51, 65–79.

Wang, Z.H., Zhen, Y.Y., Zhang, Y.D., and Wu, R.C., 2016, Review of the Ordovician conodont biostratigraphy in the different facies of North China. Journal of Stratigraphy, 40, 1–16. (in Chinese with English abstract)

Weller, J.M., 1944, Outline of Chinese geology. American Association of Petroleum Geologists Bulletin, 28, 1417–1429.

Woo, K.S., 1999, Cyclic tidal successions of the Middle Ordovician Maggol Formation in the Taebaeg area, Kangwondo, Korea. Geosciences Journal, 3, 123–140.

Wright, V.P., 1983, A rendzina from the Lower Carboniferous of South Wales. Sedimentology, 30, 159–179.

Xue, C., Dai, S., Chen, Z., and Wang, W., 2021, Research progress of Ordovician conodont biostratigraphy in Asia. Advances in Earth Science, 36, 29–44. (in Chinese with English abstract)

Zhang, S. and Barnes, C.R., 2004, Late Cambrian and Early Ordovician conodont communities from platform and slope facies, western Newfoundland: a statistical approach. The Palynology and Micropalaeontology of Boundaries, 230, 47–72.

Zhang, S.X. and Zhen, Y.Y., 1991, China. In: Moullade, M. and Nairn, A.E.M. (eds.), The Phanerozoic Geology of the World I, the Palaeozoic A. Elsevier, Amsterdam, p. 219–274.

Zhang, Y., Zhan, R., Zhen, Y., Wang, Z., Yuan, W., Fang, X., Ma, X., and Zhang, J., 2019, Ordovician integrative stratigraphy and timescale of China. Science China Earth Sciences, 62, 61–88.

Zhen, Y.Y. and Nicoll, R.S., 2009, Biogeographic and biostratigraphic implications of the *Serratognathus bilobatus* Fauna (Conodonta) from the Emanuel Formation (Early Ordovician) of the Canning Basin, western Australia. Records of the Australian Museum, 61, 1–30.

Zhen, Y.Y., Percival, I.G., and Zhang, Y.D., 2015, Floian (Early Ordovician) conodont-based biogeograpgy and biostratigraphy of the Australasian Superprovince. Palaeoworld, 24, 100–109.

Zhen, Y.Y., Zhang, Y., and Wang, Z., 2016, Huaiyuan Epeirogeny-Shaping Ordovician stratigraphy and sedimentation on the North China Platform. Palaeogeography, Palaeoclimatology, Palaeoecology, 448, 363–370.

https://doi.org/10.1007/s12303-022-0018-x